

Reconstruction of the Fermi surface and the anisotropic excitation gap of $\text{Na}_{0.5}\text{CoO}_2$

Toshiyuki Arakane,¹ Takafumi Sato,¹ Takashi Takahashi,^{1,2} Takenori Fujii,³ and Atsushi Asamitsu³

¹*Department of Physics, Tohoku University, Sendai 980-8578, Japan*

²*WPI Research Center, Advanced Institute for Materials Research, Tohoku University, Sendai 980-8577, Japan*

³*Cryogenic Center, University of Tokyo, Tokyo 113-0032, Japan*

(Received 8 June 2009; published 5 August 2009)

We have performed high-resolution angle-resolved photoemission spectroscopy of $\text{Na}_{0.5}\text{CoO}_2$ to elucidate the origin of the two-step phase transition at $T_{c1}=88$ K and $T_{c2}=53$ K. At well below T_{c2} , we find anisotropic energy-gap opening on the remnant Fermi surface (FS). This gap does not disappear at the metal-insulator transition temperature T_{c2} and survives up to T_{c1} . The remnant FS below T_{c2} shows a deviation from the normal-state FS above T_{c1} , suggesting a possible reconstruction of FS caused by the magnetic ordering.

DOI: [10.1103/PhysRevB.80.081101](https://doi.org/10.1103/PhysRevB.80.081101)

PACS number(s): 71.18.+y, 71.30.+h, 73.20.At, 71.20.Be

Since the discovery of superconductivity in hydrated cobalt oxides ($\text{Na}_x\text{CoO}_2 \cdot y\text{H}_2\text{O}$, $T_c \sim 5$ K),¹ intensive theoretical and experimental studies have been performed to elucidate the physical properties and their relation to the superconductivity. It is known that Na_xCoO_2 shows a complicated phase diagram with a variety of ground states such as the magnetic ordering and the spin density wave (SDW) as a function of Na concentration.²⁻⁴ In particular, $\text{Na}_{0.5}\text{CoO}_2$ has attracted a special attention because it shows an anomalous two-staged phase transition at $T_{c1}=88$ K and $T_{c2}=53$ K, where the magnetic susceptibility shows a sudden jump at T_{c1} and the metal-insulator transition (MIT) takes place at T_{c2} . Neutron scattering experiments have revealed the presence of superlattice spots below T_{c1} , suggestive of the 2×2 antiferromagnetic (AF) ordering in the CoO_2 plane.^{5,6} An infrared spectroscopy experiment reported that an energy gap opens below T_{c2} , consistent with the charge-density-wave (CDW) formation⁷ as also suggested by a Raman scattering experiment.⁸ NMR experiments^{9,10} observed the splitting of ^{57}Co signal below T_{c2} , indicative of one-dimensional charge inhomogeneity in the CoO_2 plane, although its relation to the MIT has not been well understood. Angle-resolved photoemission spectroscopy (ARPES) of a related compound $\text{K}_{0.5}\text{CoO}_2$ (Ref. 11) reported an anisotropic energy-gap opening at low temperatures, proposing that the MIT originates in the particle-hole instability on the Fermi surface (FS) induced by crystallization of the alkali-metal layer,¹¹ whereas the evolution of electronic states upon two-staged phase transition of $\text{Na}_{0.5}\text{CoO}_2$ as well as microscopic origin of these transitions has not been well understood.

In this paper, we report our ARPES results on $\text{Na}_{0.5}\text{CoO}_2$. We have determined the accurate k -dependence of the energy gap below T_{c2} and its temperature evolution. We found that the remnant FS of the insulating phase below T_{c2} shows a marked deviation from the FS of other doping levels as well as the calculated normal-state FS, suggesting the reconstruction of the electronic structure due to the magnetic ordering.

High-quality single crystals of Na_xCoO_2 were grown by the floating zone method. We measured the electrical resistivity and confirmed the apparent upturn below $T_{c2}=53$ K indicative of the MIT as in previous studies.² ARPES measurements were performed with a VG-SCIENIA SES2002

spectrometer at beamline BL28A at Photon Factory. We used circularly polarized lights of $h\nu=65$ and 100 eV to excite photoelectrons. The energy and angular resolutions were set at 20–40 meV and 0.2° , respectively. A clean surface was obtained by *in situ* cleaving in an ultrahigh vacuum of better than 1×10^{-10} Torr and no degradation of the sample surface was observed during the measurement. The Fermi level (E_F) of sample was referenced to that of a gold film evaporated onto the sample substrate.

Figure 1 shows the plot of ARPES intensity at E_F as a function of two-dimensional wave vector for $\text{Na}_{0.5}\text{CoO}_2$ at $T=20$ and 100 K. These temperatures correspond to those below T_{c2} (53 K) and above T_{c1} (88 K), respectively. It is noted that the bright area in Fig. 1(b) ($T=100$ K) corresponds to the normal-state FS, while that in Fig. 1(a) ($T=20$ K) shows the “remnant” FS (Ref. 13) because we found that an energy gap opens everywhere on the remnant FS, as explained later. Theoretical FS calculated by the local density approximation (LDA) (Ref. 12) is superimposed on the experimental result in Fig. 1(b). Comparison with the calculation suggests that the observed large FS centered at Γ (A) point is assigned to the hexagonal holelike a_{1g} FS in the calculation, while the theoretically predicted small e'_g FS located at K(H) point is not seen in the experiment. These experimental results are essentially consistent with previous ARPES studies.^{11,14} Although the remnant FS at 20 K looks similar to the normal-state FS at 100 K in the sense that both are a large holelike FS centered at Γ (A) point, the shape appears to be different from each other. The remnant FS looks to be rotated by 30° with respect to the calculated FS as seen in Figs. 1(a) and 1(b). This is most evident from the experimental fact that the remnant FS has a corner of hexagon in the Γ K(AH) direction while the normal-state FS is rather rounded and the hexagonlike shape is less visible. This anomalous rotation of FS with respect to the calculated FS is discussed later in detail. To demonstrate the energy-gap opening on the remnant FS, we show in Fig. 1(c) a set of ARPES spectra measured at 20 K along a cut shown by an arrow in Fig. 1(a). As seen in Fig. 1(c), a dispersive a_{1g} band rapidly approaches E_F and turns back again toward higher binding energy before reaching E_F . This behavior is highlighted in Fig. 1(d), where the second-derivative intensity of ARPES spectra is plotted as a function of wave vector and

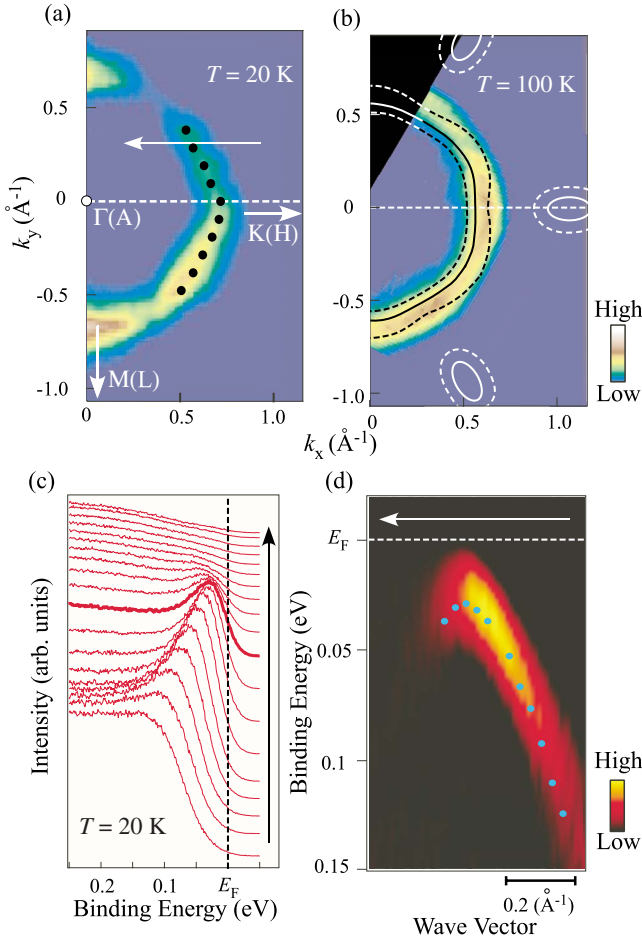


FIG. 1. (Color online) (a) Plots of ARPES intensity at E_F as a function of k_x and k_y measured with $h\nu=100$ eV at $T=20$ K for $\text{Na}_{0.5}\text{CoO}_2$. The ARPES intensity is integrated over the energy range of ± 2 meV with respect to E_F . (b) Same as (a) but at $T=100$ K. Calculated FSs by LDA (Ref. 12) at $k_z=0$ (dashed line) and $k_z=0.5\pi$ (solid lines) are also shown for comparison. (c) ARPES spectra of $\text{Na}_{0.5}\text{CoO}_2$ measured along a cut shown in (a). (d) Second-derivative intensity of ARPES spectra in (c) as a function of binding energy and wave vector. Open circles denote the energy position of a quasiparticle peak determined by tracing the peak position of EDCs.

binding energy. We clearly recognize a backfolding of the band, as observed in various CDW materials.¹⁵

To illustrate the momentum dependence of the energy gap below T_{c2} , we show in Fig. 2(a) ARPES spectra at various k_F points in the BZ shown by colored circles in Fig. 2(b). We find that a well-defined peak appears near E_F for all k_F points and its energy position shows a systematic momentum dependence indicative of an anisotropic nature of the energy gap, as reported also in $\text{K}_{0.5}\text{CoO}_2$.¹¹ In order to estimate the gap size, we have divided each ARPES spectrum by the Fermi-Dirac (FD) function at 20 K convolved with the instrumental resolution. The result is shown in Fig. 2(c). As indicated by the open circles, the energy position of peak, reflecting the gap size, varies significantly with momentum. A smallest gap of 20 meV is seen at points C and D while a relatively large gap of 60 meV opens at points H and I. We plot in Fig. 2(d) the peak position and the shift of leading-

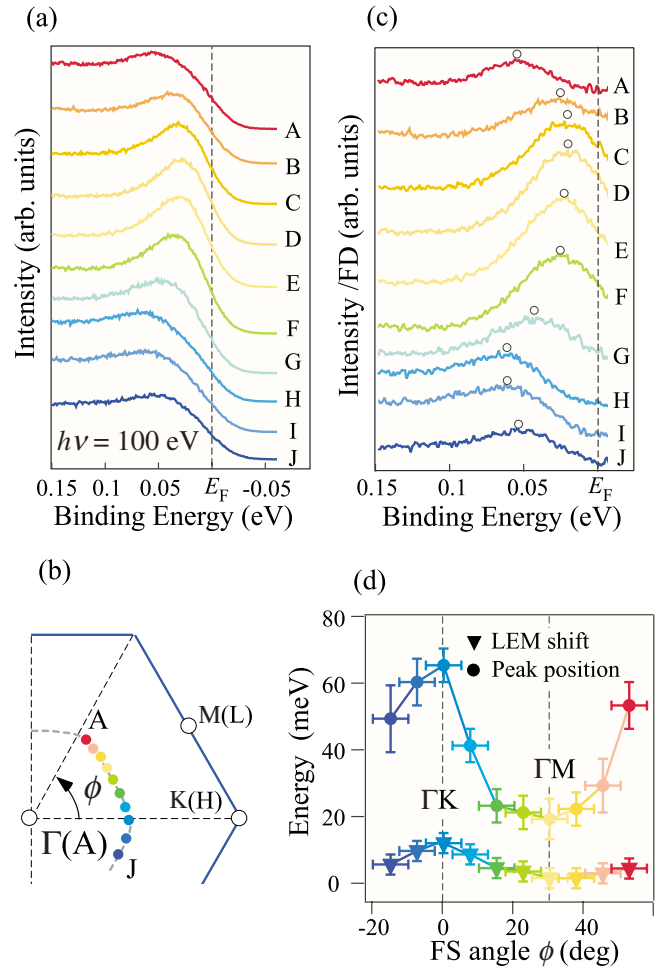


FIG. 2. (Color online) (a) Near- E_F ARPES spectra of $\text{Na}_{0.5}\text{CoO}_2$ measured at $T=20$ K at various k_F points shown on the FS in (b). Coloring of the spectrum is the same as that of circles in (b). Location of k_F points of the a_{1g} band (solid circles) together with the definition of the FS angle (ϕ) is shown in (b). (c) ARPES spectra divided by the FD function at 20 K convolved with a Gaussian reflecting the instrumental resolution. (d) Energy position of a peak in (c) reflecting the gap size (blue circles) together with the LEM shift (red circles) as a function of the FS angle (ϕ).

edge midpoint (LEM) relative to E_F as a function of the FS angle ϕ by the blue and red circles, respectively. It is clear from Fig. 2(d) that the energy gap shows a distinct anisotropy with the minimum and maximum in ΓM and ΓK directions, respectively.

Figures 3(a) and 3(b) show the temperature dependence of ARPES spectrum near E_F measured at two representative k_F points ($\phi=0^\circ$ and 30°). As seen in the figures, the LEM gradually moves toward E_F with increasing temperature and finally reaches E_F at around 100 K for both k_F points. This is better illustrated in Fig. 3(d), where we plot the energy position of LEM relative to E_F as a function of temperature. We find that the LEM shift is quite remarkable at $T=20$ –80 K, but looks to be saturated at $T=90$ –100 K. The persistence of the gradual shift of LEM even in the metallic phase of $T_{c2}(53 \text{ K}) < T < T_{c1}(88 \text{ K})$ suggests that there is a pseudogap in the metallic phase. It is also remarked that the

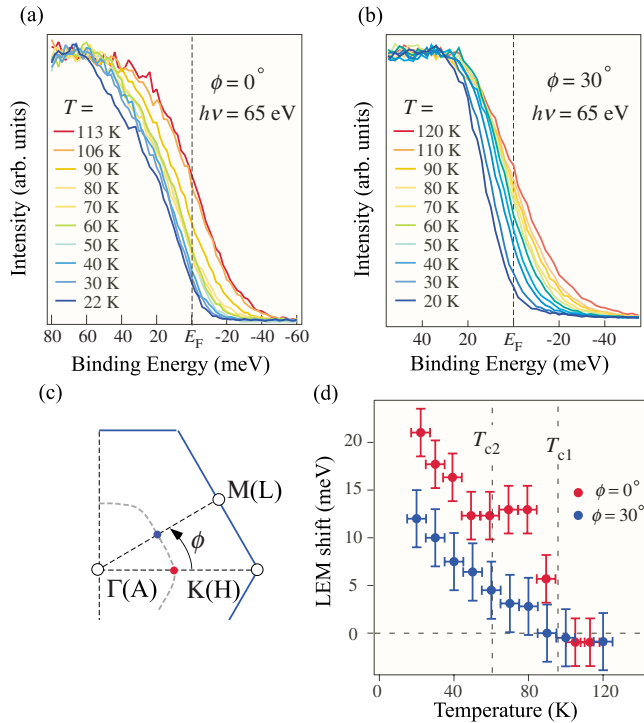


FIG. 3. (Color online) Temperature dependence of ARPES spectrum measured on the FS (a) and (b) at $\phi=0^\circ$ (red/gray circle) and 30° (blue/dark gray circle), respectively, as shown in (c). (d) Temperature dependence of LEM shift for $\phi=0$ and 30° .

LEM shift at $\phi=0^\circ$ shows a plateau at $T_{c2} < T < T_{c1}$, suggesting that the LEM-shift value is correlated with both T_{c2} and T_{c1} .¹⁶

Now we discuss the origin of the unconventional shape of the remnant FS below T_{c2} shown in Fig. 1(a). Possible candidates to explain the anomalous shape of the remnant FS and the energy-gap opening would be (i) the CDW caused by nesting of the parallel segment of a_{1g} FS as shown in Fig. 4(a), (ii) the charge ordering of Na^+ ions,¹⁷ (iii) the magnetic ordering or the SDW, and (iv) the combination of these effects. The possible scenario (i) may be unlikely since the samples with other doping levels do not show a phase transition whereas the parallel segments of FS still remains. As for the scenario (ii), $2 \times \sqrt{3} \text{Na}^+$ charge order defines a new rectangular BZ [blue dashed line in Fig. 4(b)]. The original FS is folded [gray solid lines in Fig. 4(b)] with respect to this reconstructed BZ to create several small FSs [solid blue curves in Fig. 4(b)] due to a finite hybridization between the original and the folded bands. In this case, the expected reconstructed FS shows a mirror symmetry with respect to the vertical line along the ΓM cut [orange line in Fig. 4(b)] but do not appear to show the 30° -rotation behavior unlike the present experiment [Fig. 1(a)].

In relation to the scenario (iii), it is remarked that the 2×2 magnetic ordering has been observed below T_{c1} by neutron scattering experiments.⁵ The 2×2 magnetic ordering forms a magnetic BZ which has a shape exactly the same as the original BZ but shrinks by 50%, as shown by the red dashed line in Fig. 4(c). The original FS is folded with respect to this magnetic BZ [gray lines in Fig. 4(c)], and the

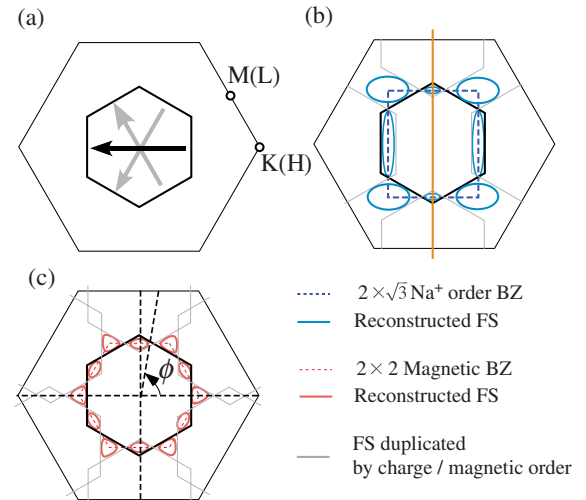


FIG. 4. (Color online) Schematic view of the FS reconstruction. (a) Simple nesting case where the parallel segments of the normal-state FS (black line) are connected with each other. (b) Na^+ -order-induced FS reconstruction. Normal-state FS (black line) is folded (gray line) with respect to the reconstructed BZ (blue dashed line) reflecting the $2 \times \sqrt{3} \text{Na}^+$ order. Expected FSs with the finite hybridization of bands are shown by solid light blue curves. (c) Magnetic-order-induced FS reconstruction. Normal-state FS (black line) is folded (gray line) with respect to the reconstructed BZ (dashed red line) with the 2×2 magnetic potential. Expected FSs with the finite hybridization of bands are shown by solid red curves.

hybridization between the original and folded FSs would produce several disconnected FSs as shown by red curves in Fig. 4(c). Taking into account a finite momentum broadening, we expect that the overall shape of FS shows a good agreement with the present ARPES experiment in Fig. 1(a). In this sense, the rounded shape of the 100 K FS would be a fingerprint of strong magnetic fluctuations even above T_{c1} . We think that the character of energy gap in Fig. 3 is also related to this magnetic ordering picture. As shown in Fig. 3, the temperature dependence of the energy gap along the ΓK and ΓM directions appears to reflect the T_{c1} (88 K) and T_{c2} (53 K) instabilities, respectively. We speculate that the reason why the states along the ΓK direction are more associated with the T_{c1} instability would be due to the smaller Fermi velocity as compared to that along the ΓM direction,¹⁸ which would result in the better nesting condition of the magnetic ordering along the ΓK direction. We also note that the difference in the magnitude of the energy gap well below T_{c2} along two directions [Fig. 3(d)] is not satisfactorily understood by the simple magnetic ordering scenario, suggesting that another mechanism is at work. As for a possible mechanism, (i) cooperation of the magnetic ordering and the Na^+ charge ordering and/or (ii) possible influences from the FS nesting would be considered, while we leave this point as an open question.

Finally, we compare the present results with other experiments. An optical spectroscopy measurement⁷ reported the existence of an energy gap of ~ 15 meV, which may basically reflect the smallest gap in ARPES. The electrical resistivity measurement^{2,19} shows an insulatinglike behavior be-

low T_{c2} , consistent with the present ARPES result which shows that the energy gap opens everywhere in BZ. On the other hand, at $T_{c2} < T < T_{c1}$, the resistivity shows a metallic behavior while the finite LEM shift (pseudogap) is still observed in ARPES. This would be because the observed pseudogap has a finite density of states at E_F as shown by Figs. 3(a) and 3(b).

In conclusion, we have reported our ARPES results of $\text{Na}_{0.5}\text{CoO}_2$ to elucidate the nature of the two-step phase transition. We observed anomalous reconstruction of the electronic structure below T_{c2} . We also found a highly anisotropic energy gap below T_{c2} which does not close at the MIT

temperature T_{c2} and survives up to T_{c1} . We have concluded that the magnetic ordering plays an important role for the energy gap and the remnant FS below T_{c2} .

We thank K. Nakayama, Z.-H. Pan, Y.-M. Xu, M. Neupan, M. Kubota, and K. Ono for their help in the experiment. The authors also thank Y. Kobayashi and H. Ding for useful discussions. ARPES measurements were carried out at KEK-PF (Proposal No. 2006S2-001). This work was supported by grants from JSPS, MEXT, and CREST-JST of Japan. T.A. thanks JSPS for a financial support.

-
- ¹K. Takada, H. Sakurai, E. Takayama-Muromachi, F. Izumi, R. A. Dilanian, and T. Sasaki, *Nature (London)* **422**, 53 (2003).
²M. L. Foo, Y. Wang, S. Watauchi, H. W. Zandbergen, T. He, R. J. Cava, and N. P. Ong, *Phys. Rev. Lett.* **92**, 247001 (2004).
³S. P. Bayrakci, I. Mirebeau, P. Bourges, Y. Sidis, M. Enderle, J. Mesot, D. P. Chen, C. T. Lin, and B. Keimer, *Phys. Rev. Lett.* **94**, 157205 (2005).
⁴J. Sugiyama, J. H. Brewer, E. J. Ansaldo, H. Itahara, T. Tani, M. Mikami, Y. Mori, T. Sasaki, S. Hèbert, and A. Maignan, *Phys. Rev. Lett.* **92**, 017602 (2004).
⁵M. Yokoi, T. Moyoshi, Y. Kobayashi, M. Soda, Y. Yasui, M. Sato, and K. Kakurai, *J. Phys. Soc. Jpn.* **74**, 3046 (2005).
⁶G. Gašparović, R. A. Ott, J.-H. Cho, F. C. Chou, Y. Chu, J. W. Lynn, and Y. S. Lee, *Phys. Rev. Lett.* **96**, 046403 (2006).
⁷N. L. Wang, D. Wu, G. Li, X. H. Chen, C. H. Wang, and X. G. Luo, *Phys. Rev. Lett.* **93**, 147403 (2004).
⁸Q. Zhang, M. An, S. Yuan, Y. Wu, D. Wu, J. Luo, N. L. Wang, W. Bao, and Y. Wang, *Phys. Rev. B* **77**, 045110 (2008).
⁹M. Yokoi, Y. Kobayashi, T. Moyoshi, and M. Sato, *J. Phys. Soc. Jpn.* **77**, 074704 (2008).
¹⁰F. L. Ning, S. M. Golin, K. Ahilan, T. Imai, G. J. Shu, and F. C. Chou, *Phys. Rev. Lett.* **100**, 086405 (2008).
¹¹D. Qian, L. Wray, D. Hsieh, D. Wu, J. L. Luo, N. L. Wang, A. Kuprin, A. Fedorov, R. J. Cava, L. Viciu, and M. Z. Hasan, *Phys. Rev. Lett.* **96**, 046407 (2006).
¹²D. J. Singh, *Phys. Rev. B* **61**, 13397 (2000).
¹³F. Ronning, C. Kim, D. L. Feng, D. S. Marshall, A. G. Loeser, L. L. Miller, J. N. Eckstein, I. Bozovic, and Z.-X. Shen, *Science* **282**, 2067 (1998).
¹⁴H.-B. Yang, Z.-H. Pan, A. K. P. Sekharan, T. Sato, S. Souma, T. Takahashi, R. Jin, B. C. Sales, D. Mandrus, A. V. Fedorov, Z. Wang, and H. Ding, *Phys. Rev. Lett.* **95**, 146401 (2005).
¹⁵L. Perfetti, T. A. Gloor, F. Mila, H. Berger, and M. Grioni, *Phys. Rev. B* **71**, 153101 (2005).
¹⁶We note that the LEM-shift values between Figs. 2(d) and 3(d) are different due to difference in the energy resolution (40 and 20 meV, respectively).
¹⁷H. W. Zandbergen, M. L. Foo, Q. Xu, V. Kumar, and R. J. Cava, *Phys. Rev. B* **70**, 024101 (2004).
¹⁸J. Geck, S. V. Borisenko, H. Berger, H. Eschrig, J. Fink, R. Follath, M. Knupfer, A. Koitzsch, A. A. Kordyuk, V. B. Zabolotnyy, and B. Büchner, *Phys. Rev. Lett.* **99**, 046403 (2007).
¹⁹H. Watanabe, Y. Mori, M. Yokoi, T. Moyoshi, M. Soda, Y. Yasui, Y. Kobayashi, M. Sato, N. Igawa, and K. Kakurai, *J. Phys. Soc. Jpn.* **75**, 034716 (2006).